Outline: Peripheral collisions

Lecturer: Hans-Jürgen Wollersheim

e-mail: h.j.wollersheim@gsi.de

web-page: https://web-docs.gsi.de/~wolle/ and click on

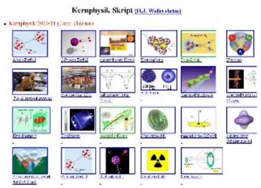

1. reaction Q-value
2. sub-barrier transfer reactions
3. transfer probabilities for multi-nucleon transfer
4. PRISMA and HIRA spectrometers
5. transfer reactions with weakly bound nuclei

Peripheral collisions

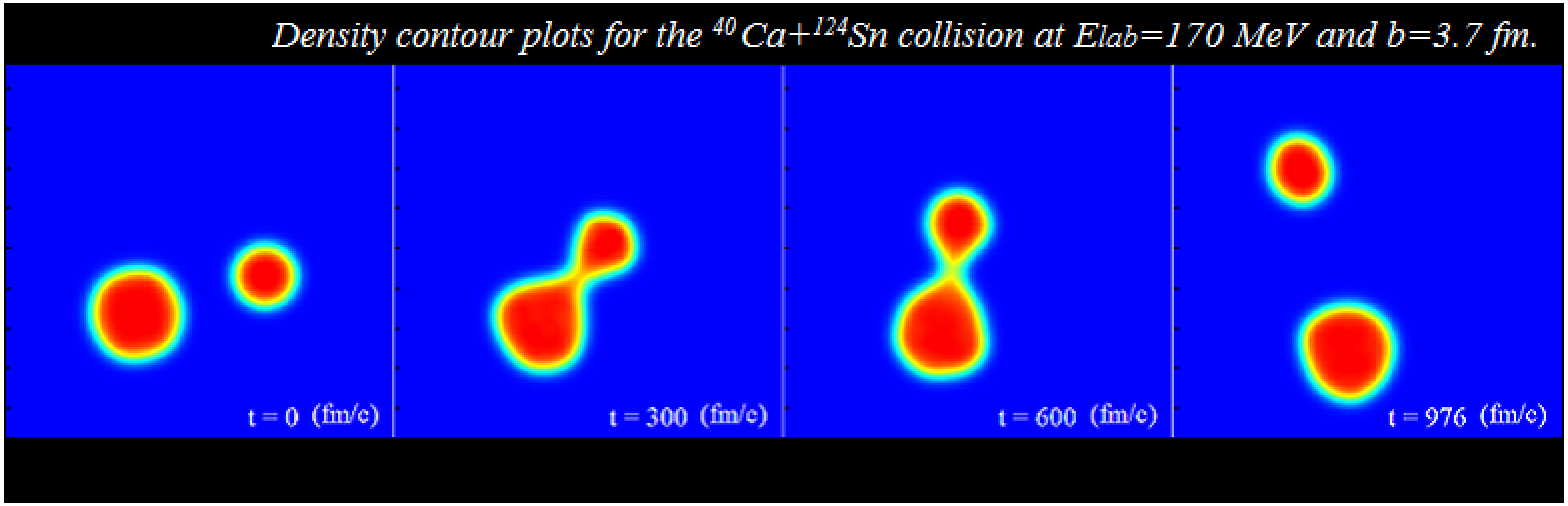

- probing single particle aspects and nucleon-nucleon correlations
- transition from quasi elastic to deep inelastic processes
- connection with other reaction channels (near and sub-barrier fusion)
- population of neutron-rich nuclei

time-dependent density functional theory

Peripheral collisions

Sub-barrier transfer reactions
study of nucleon-nucleon correlations

Multi-nucleon transfer
study of secondary processes

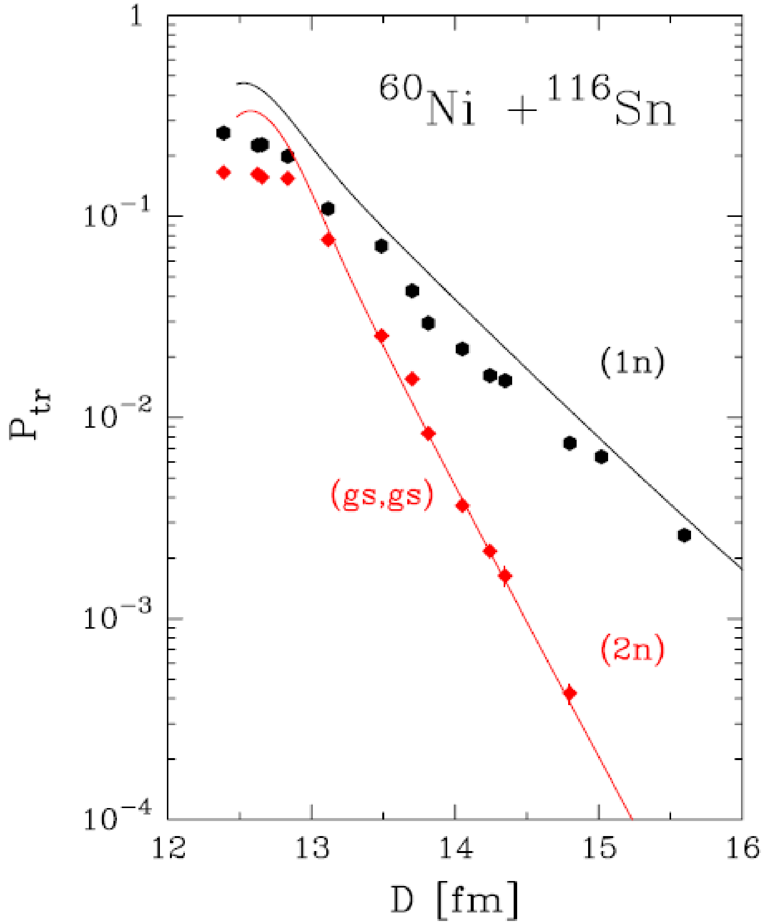

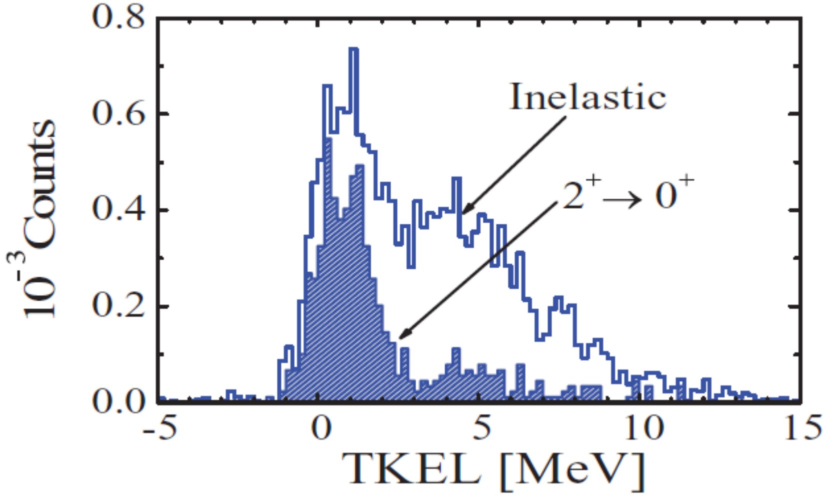

C_p = 4.2 fm, C_t = 5.5 fm, R_{int} = 12.7 fm

Reaction Q-value

Consider the T(p,x)R reaction:

The *Q-value* of the reaction is defined as the difference in mass energies of the products and reactants, i.e.

$$Q_{gg} = \left[m_p + m_t - (m_x + m_R)\right] \cdot c^2$$

if Q is positive, the reaction is **exoergic** while if Q is negative, the reaction is **endoergic**.

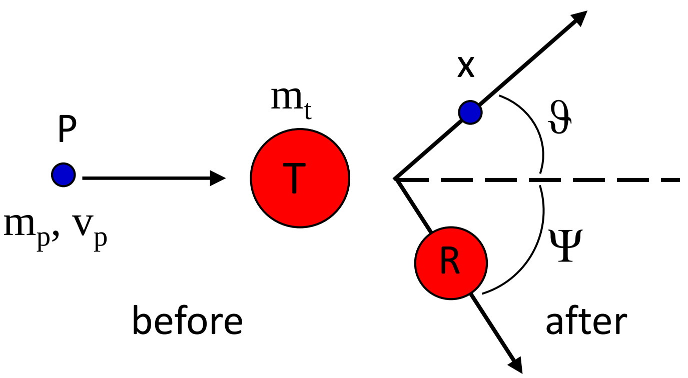

https://www.nndc.bnl.gov/qcalc/

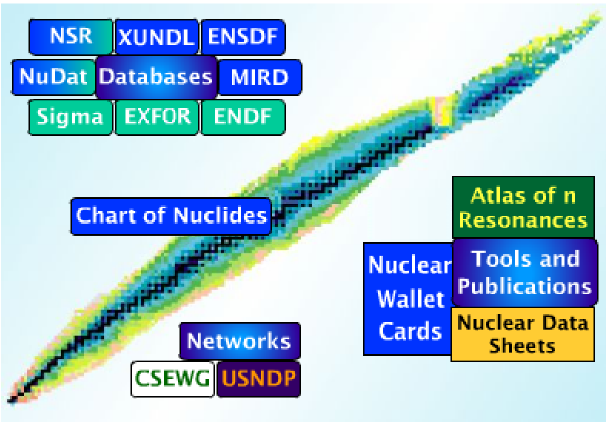

$$m_p c^2 + T_p + m_t c^2 = m_x c^2 + T_x + m_R c^2 + T_R$$

$$Q_{gg} = \left[m_p + m_t - m_x - m_R\right] c^2 = T_x + T_R - T_p$$

Reaction Q-value

Consider the T(p,x)R reaction:

The *Q-value* of the reaction is defined as the difference in mass energies of the products and reactants, i.e.

$$Q_{gg} = \left[m_p + m_t - (m_x + m_R)\right] \cdot c^2$$

if Q is positive, the reaction is **exoergic** while is Q is negative, the reaction is **endoergic**.

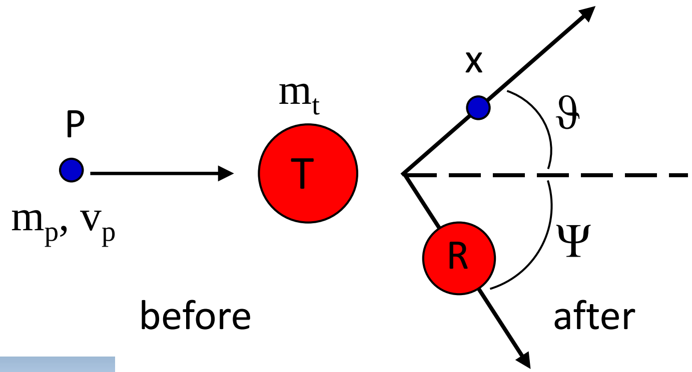

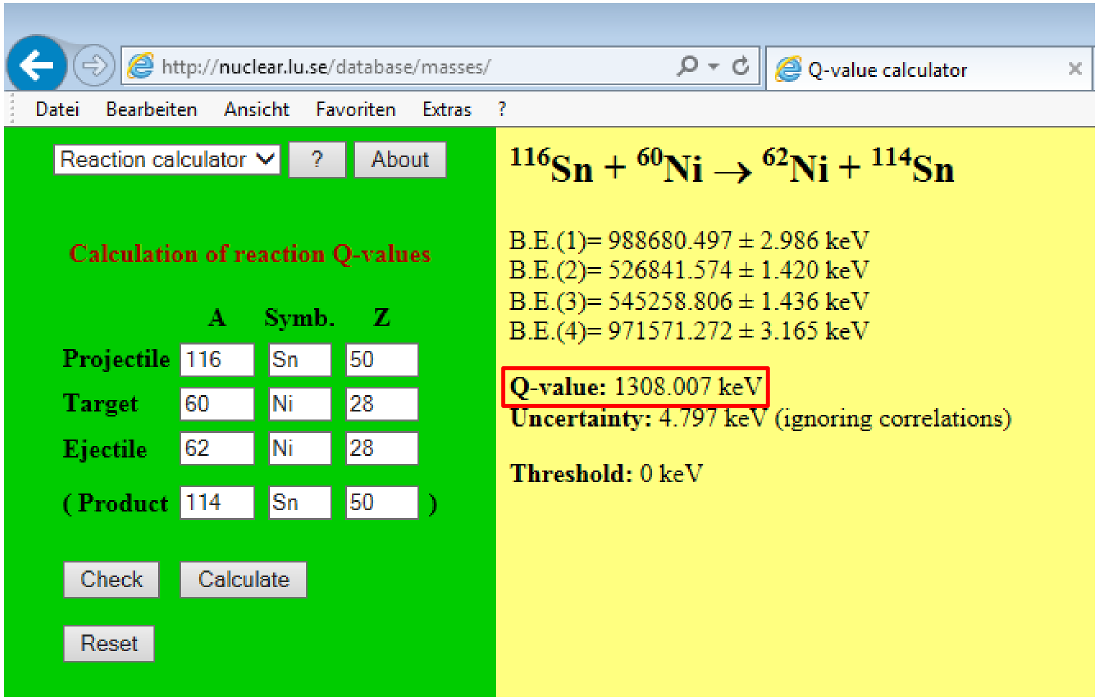

Reaction Q-value neutron transfer

Consider the T(p,x)R reaction:

The *Q-value* of the reaction is defined as the difference in mass energies of the products and reactants, i.e.

$$Q_{gg} = [m_p + m_t - (m_x + m_R)] \cdot c^2$$

if Q is positive, the reaction is **exoergic** while is Q is negative, the reaction is **endoergic**.

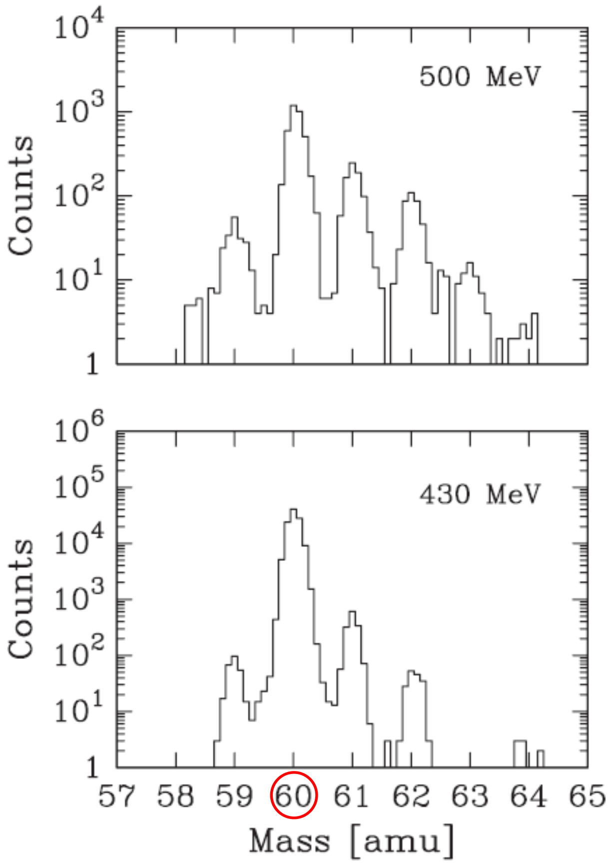

$^{116}Sn \rightarrow {}^{60}Ni$ @ E_{lab} = 430, 460, 500 MeV

E_{cm} = 147, 156, 170 MeV

$V_C(R_{int})$ = 159 MeV

(^{60}Ni,^{58}Ni) -2n	(^{60}Ni,^{59}Ni) -1n	(^{60}Ni,^{60}Ni) 0n	(^{60}Ni,^{61}Ni) +1n	(^{60}Ni,^{62}Ni) +2n	(^{60}Ni,^{63}Ni) +3n	(^{60}Ni,^{64}Ni) +4n
-4,12 MeV	-4.44 MeV	0 MeV	-1.74 MeV	+1.31 MeV	-2.15 MeV	-0.24 MeV

Reaction Q-value proton transfer

Consider the T(p,x)R reaction:

The *Q-value* of the reaction is defined as the difference in mass energies of the products and reactants, i.e.

$$Q_{gg} = \left[m_p + m_t - (m_x + m_R)\right] \cdot c^2$$

if Q is positive, the reaction is **exoergic** while is Q is negative, the reaction is **endoergic**.

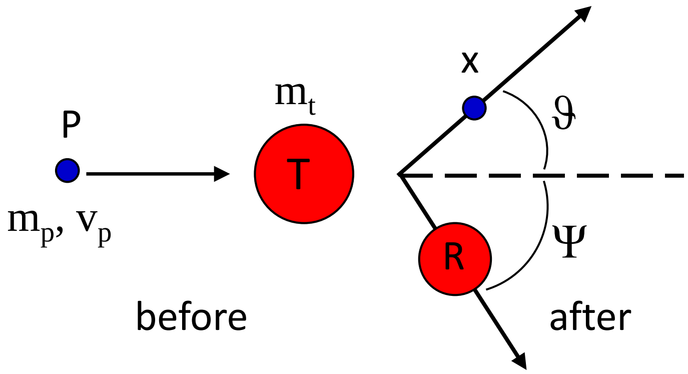

The Q-value of the reaction will change for **proton transfer** due to the rearrangement of nuclear charge.

$$Q_{opt} = Q_{gg} - E^* = Q_{gg} - e^2\left[\frac{Z_pZ_t}{r_i} - \frac{(Z_p - z)(Z_t + z)}{r_f}\right]$$

$$Q_{opt} = Q_{gg} - \frac{Z_pZ_te^2}{r_i} \cdot \left[1 - \frac{(Z_p - z)(Z_t + z)}{Z_pZ_t}\frac{r_i}{r_f}\right]$$

$$r_i = D = \frac{0.72 \cdot Z_1Z_2}{E_{cm}}\left[sin^{-1}\frac{\theta_{cm}}{2} + 1\right]$$

$$Q_{opt} = Q_{gg} - \frac{2E_{cm}}{\left[sin^{-1}\frac{\theta_{cm}}{2} + 1\right]} \cdot \left[1 - \frac{(Z_p - z)(Z_t + z)}{Z_pZ_t}\frac{r_i}{r_f}\right]$$

$$Q_{opt} \approx Q_{gg} - E_{cm} \cdot \left[1 - \frac{(Z_p - z)(Z_t + z)}{Z_pZ_t}\right]$$

Reaction Q-value

The population in the (N,Z) plane is governed by Q_{opt}

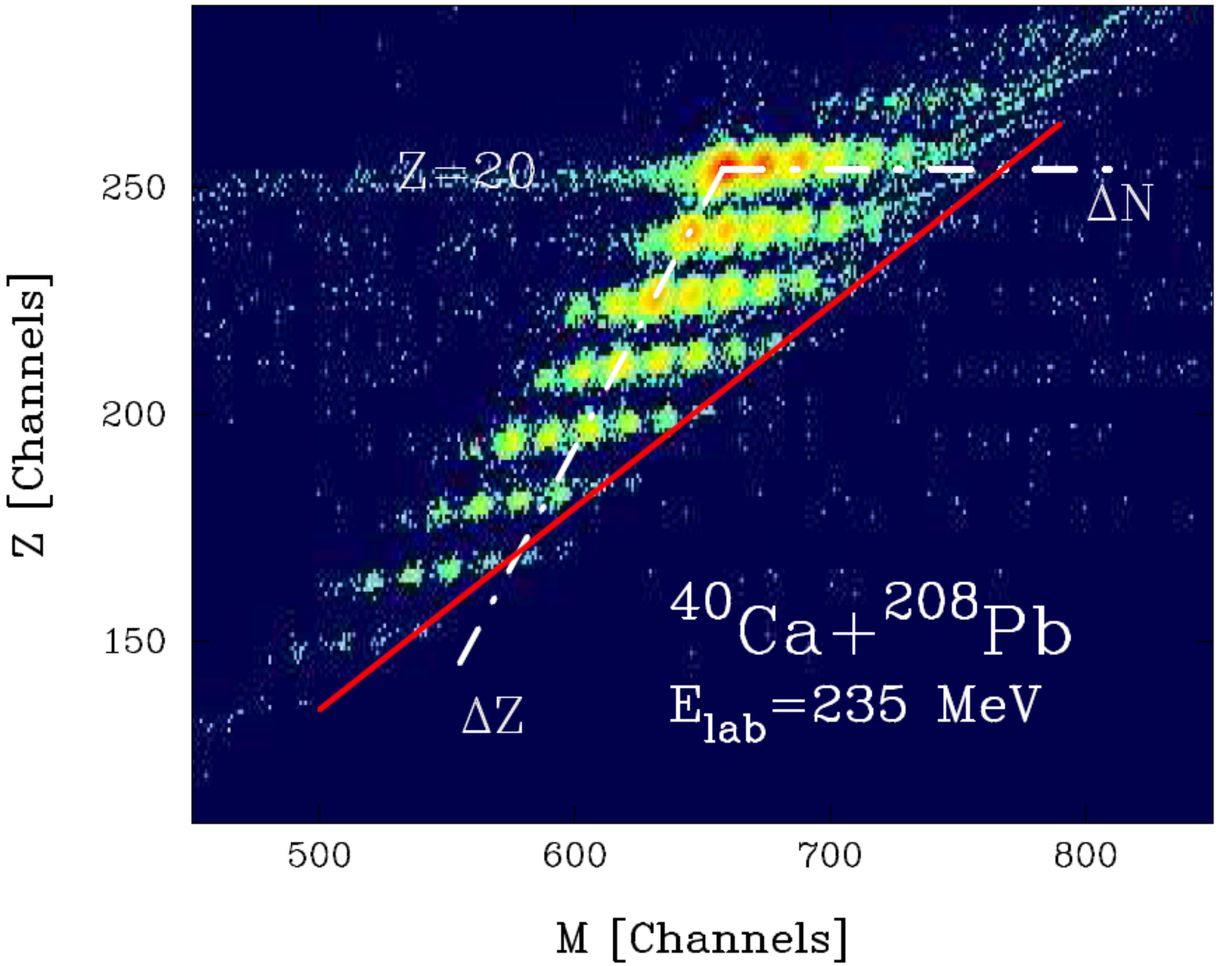

E_{cm} = 197 MeV $V_C(R_{int})$ = 178 MeV

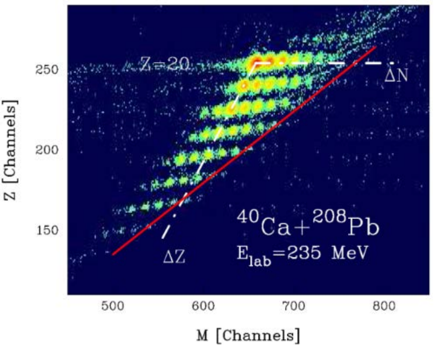

Reaction Q-value

The population in the (N,Z) plane is governed by Q_{opt}

	E^*
$_{22}$Ti	-14.4
$_{21}$Sc	-7.3
$_{20}$Ca	0
$_{19}$K	+7.6
$_{18}$Ar	+15.4
$_{17}$Cl	+23.4
$_{16}$S	+31.7
$_{15}$P	+40.3
$_{14}$Si	+49.0

$E_{cm}\cdot[1-V_C(f)/V_C(i)]$ (MeV)

Q_{gg} (MeV)

$[V_C(i)-V_C(f)]$ (MeV)

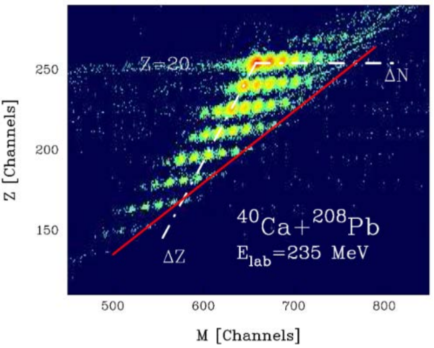

Reaction Q-value

The population in the (N,Z) plane is governed by Q_{opt}

	E^*	-2n	-1n	**0n**	1n	2n	3n	4n	5n	6n	7n	8n
$_{22}$Ti	-14.4	-47.7	-37.4	-23.0	-17.2	-6.3	-3.9	+3.5	+4.9	+10.5	+10.8	+15.4
$_{21}$Sc	-7.3	0.0	-25.9	-13.2	-8.3	-2.4	+0.1	+4.9	+6.1	+10.1	+10.3	+13.8
$_{20}$**Ca**	0	-20.4	-12.0	0	+1.3	+6.2	+6.4	+11.1	+10.3	+14.0	+12.8	+15.9
$_{19}$K	+7.6	-13.9	-6.7	+2.1	+2.6	+6.1	+5.9	+8.7	+7.8	+9.6	+7.9	+9.0
$_{18}$Ar	+15.4	-3.2	-0.1	+7.5	+6.6	+9.8	+7.8	+10.4	+7.5	+8.9	+5.5	+6.4
$_{17}$Cl	+23.4	-1.1	+1.6	+7.2	+5.9	+7.0	+4.6	+5.4	+2.6	+2.3	-2.7	-3.1
$_{16}$S	+31.7	+4.8	+5.3	+10.4	+7.0	+8.1	+3.9	+4.6	-0.5	-1.1	-7.0	-8.1
$_{15}$P	+40.3	+4.1	+3.8	+7.0	+2.6	+2.2	-2.9	-4.0	-9.2	-12.2	-18.5	-21.4
$_{14}$Si	+49.0	+6.6	+4.1	+6.2	+0.6	-0.6	-7.2	-9.4	-16.5	-19.4	-27.4	-30.4

$E_{cm} \cdot [1-V_C(f)/V_C(i)]$ (MeV) Q_{gg} - $[V_C(i)-V_C(f)]$ (MeV)

A smooth transition between quasi-elastic and deep inelastic processes

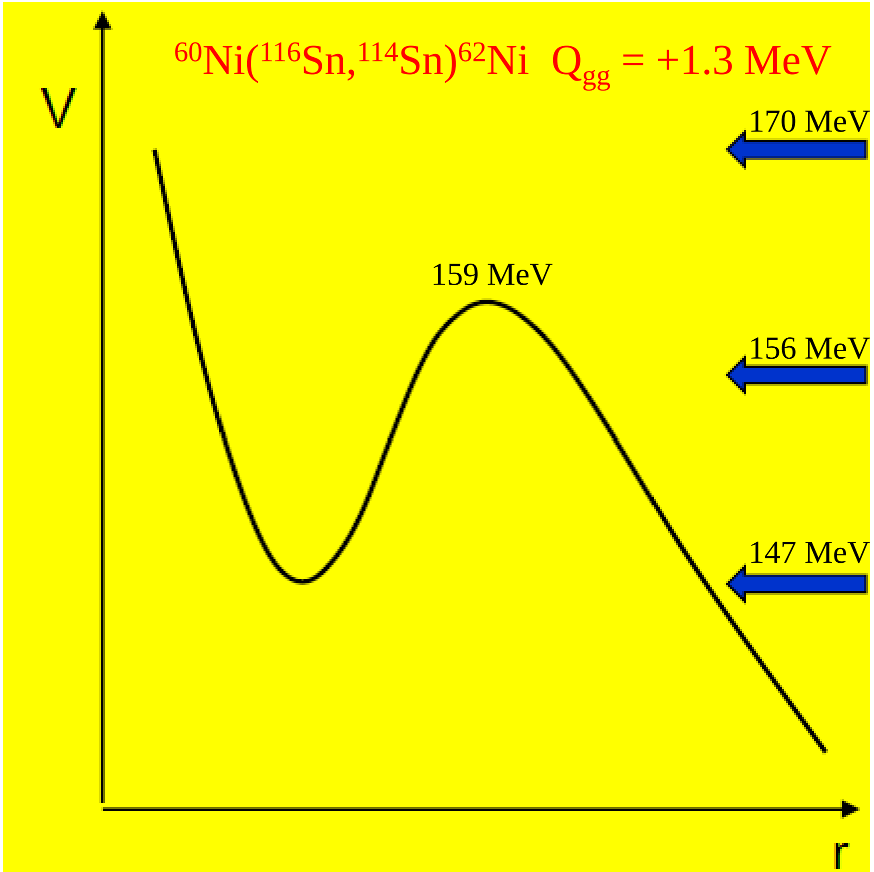

$E > E_B$

$E \sim E_B$

$E < E_B$

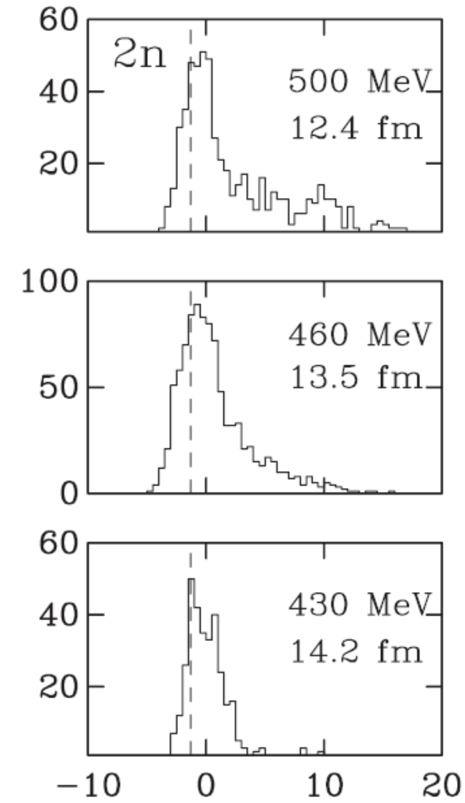

Below the barrier Q-values gets very narrow and without deep inelastic components

From quasi-elastic to deep-inelastic regime $^{90}Zr + ^{208}Pb$ at E=560 MeV (PRISMA)

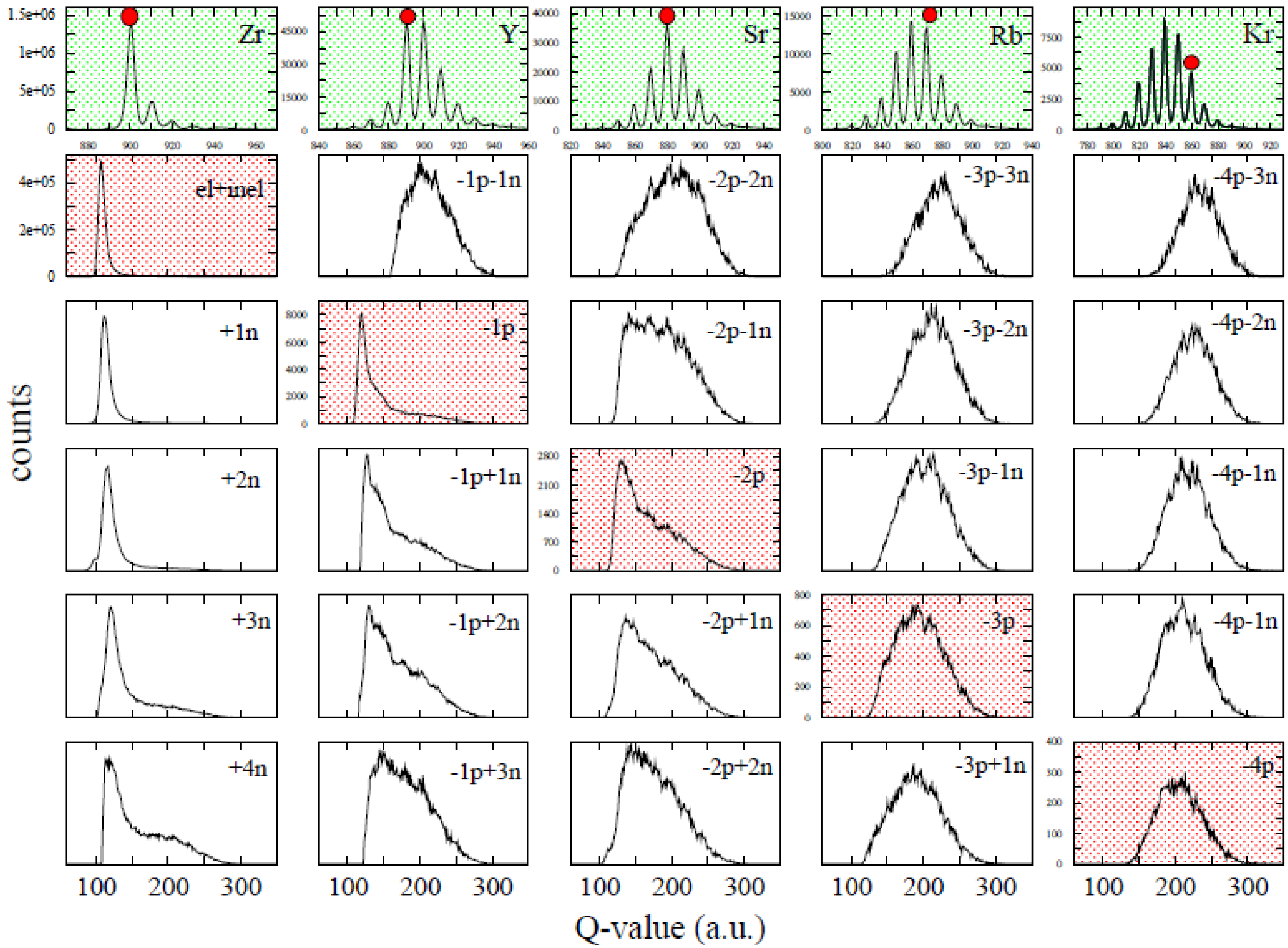

$E_{cm}/V_C(R_{int}) = 1.19$

Sub-barrier transfer reactions

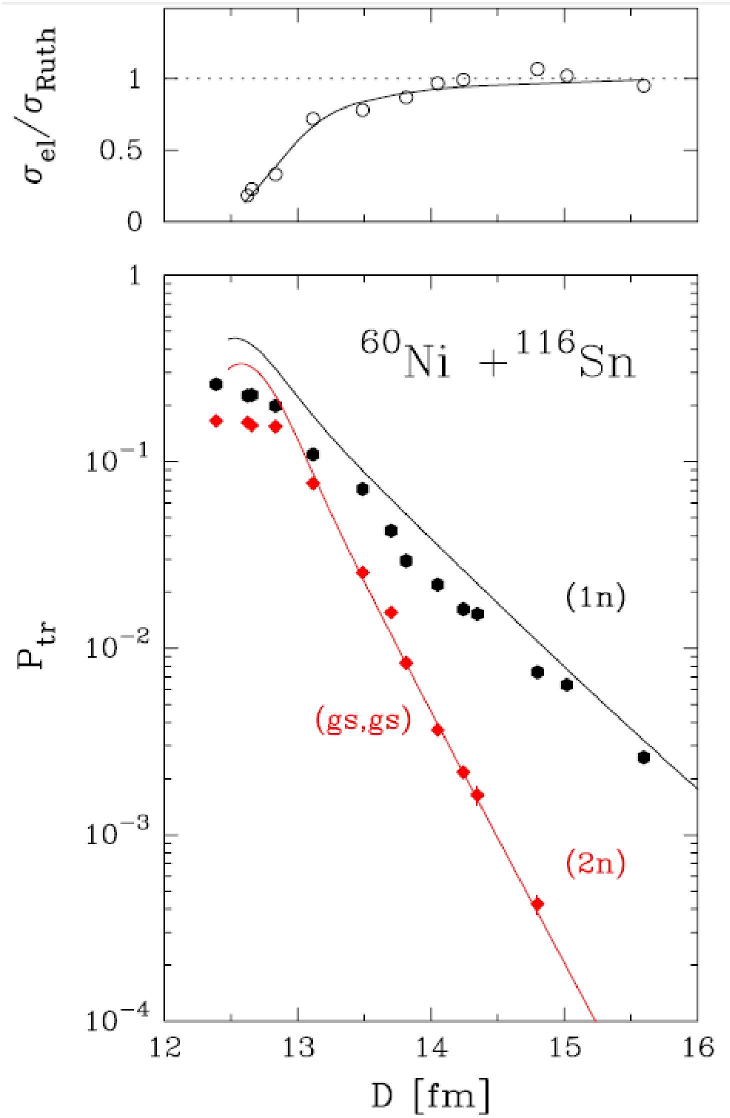

$^{60}Ni(^{116}Sn,^{114}Sn)^{62}Ni$ $Q_{gg} = +1.3$ MeV

slopes of P_{tr} versus D are expected from the binding energy

$$\frac{P_{tr}}{sin(\theta_{cm}/2)} \propto exp(-2\alpha \cdot D) \qquad \alpha = \sqrt{\frac{2\mu B}{\hbar^2}}$$

B → binding energy $\qquad \alpha_{xn}[fm^{-1}] = 0.21874\sqrt{x \cdot B_{MeV}}$

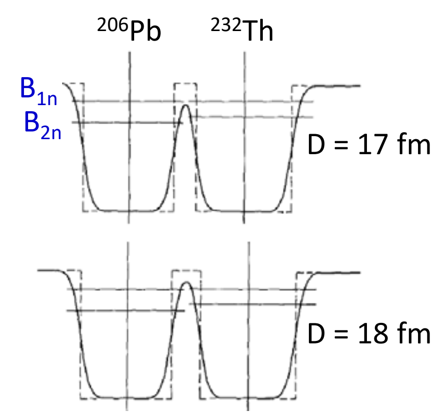

one probes tunneling effects between interacting nuclei, which enter into contact through the tail of their density distributions

$$D = \frac{Z_1 Z_2 e^2}{2E_{cm}} \cdot \left(1 + sin^{-1}(\theta_{cm}/2)\right)$$

D. Montanari et al.; Phys. Rev. Lett 113, 052501 (2014)

Inelastic scattering close to the Coulomb barrier

electromagnetic and nuclear excitation

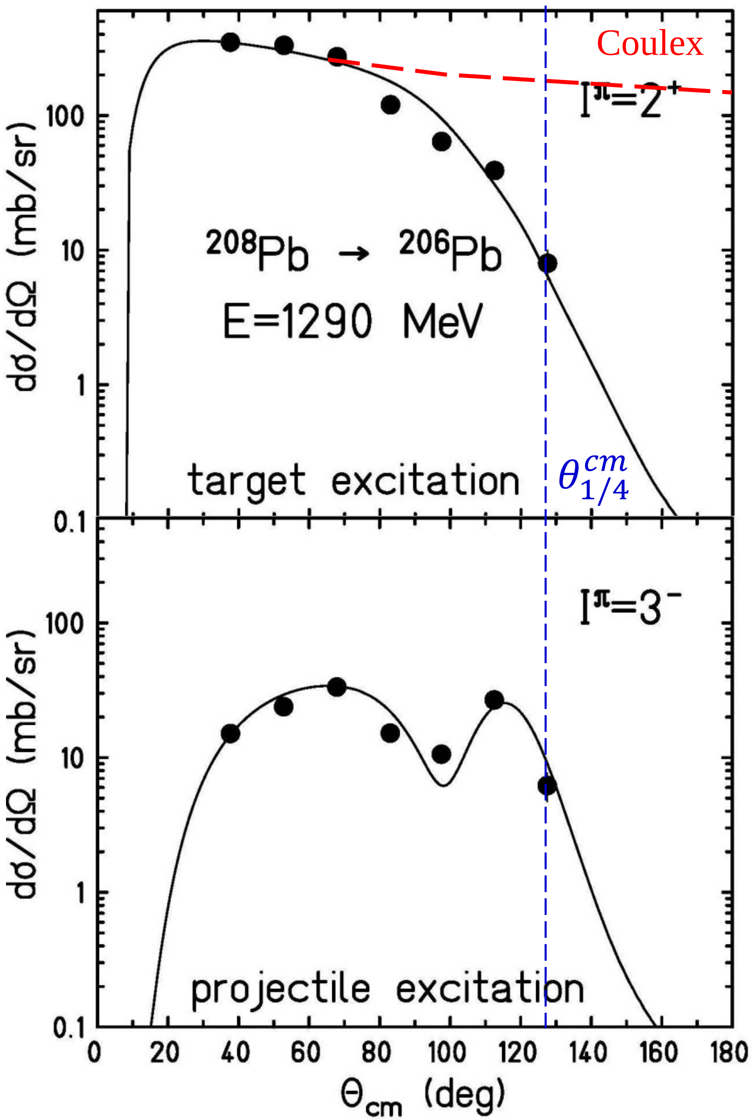

^{208}Pb + ^{206}Pb at E_{cm} = 641.7 MeV

C_p = 6.81 fm, C_t = 6.79 fm, R_{int} = 15.95 fm, $V_C(R_{int})$ = 607,0 MeV

$\theta_{1/4}^{cm} = 127.6^0$

$$\frac{d\sigma_{inel}}{d\Omega_{cm}} = \{1 - P_{abs}(D, \theta_{cm})\} \cdot \frac{d\sigma_{coul}}{d\Omega_{cm}}$$

$$\sigma_{reac} = P_{abs}(D, \theta_{cm}) \cdot \sigma_{Ruth}$$

$$[1 - P_{abs}(D)] = exp\left\{-\frac{2}{\hbar}\int_{-\infty}^{+\infty} W[r(t)]dt\right\}$$

$$W[r(t)] = W_0 \cdot exp\left[-\frac{r(t) - C_1 - C_2}{a_I}\right]$$

$$[1 - P_{abs}(D)] = exp\left\{-\frac{2}{\hbar} \cdot W_0 \cdot exp\left[-\frac{D - C_1 - C_2}{a_I}\right] \cdot \frac{D}{v}\right\}$$

Transfer studies at energies below the Coulomb barrier

✓ only a few reaction channels are open
one reduces uncertainties with nuclear potentials
✓ Q-value distributions get much narrower
one can probe nucleon correlations close to the ground state

but

1. angular distributions are backward peaked
   projectile-like particles have low kinetic energy
2. a complete identification of final reaction products in A,Z and Q-values becomes difficult
3. cross sections get very small (need for high efficiency)

solutions:

- use Recoil Mass Separator
- use Magnetic Spectrometers with inverse kinematics

Prisma spectrometer

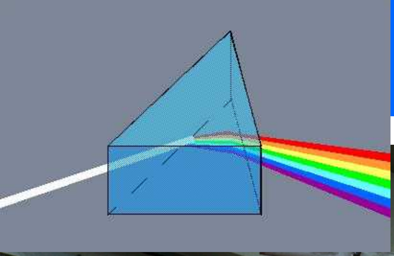

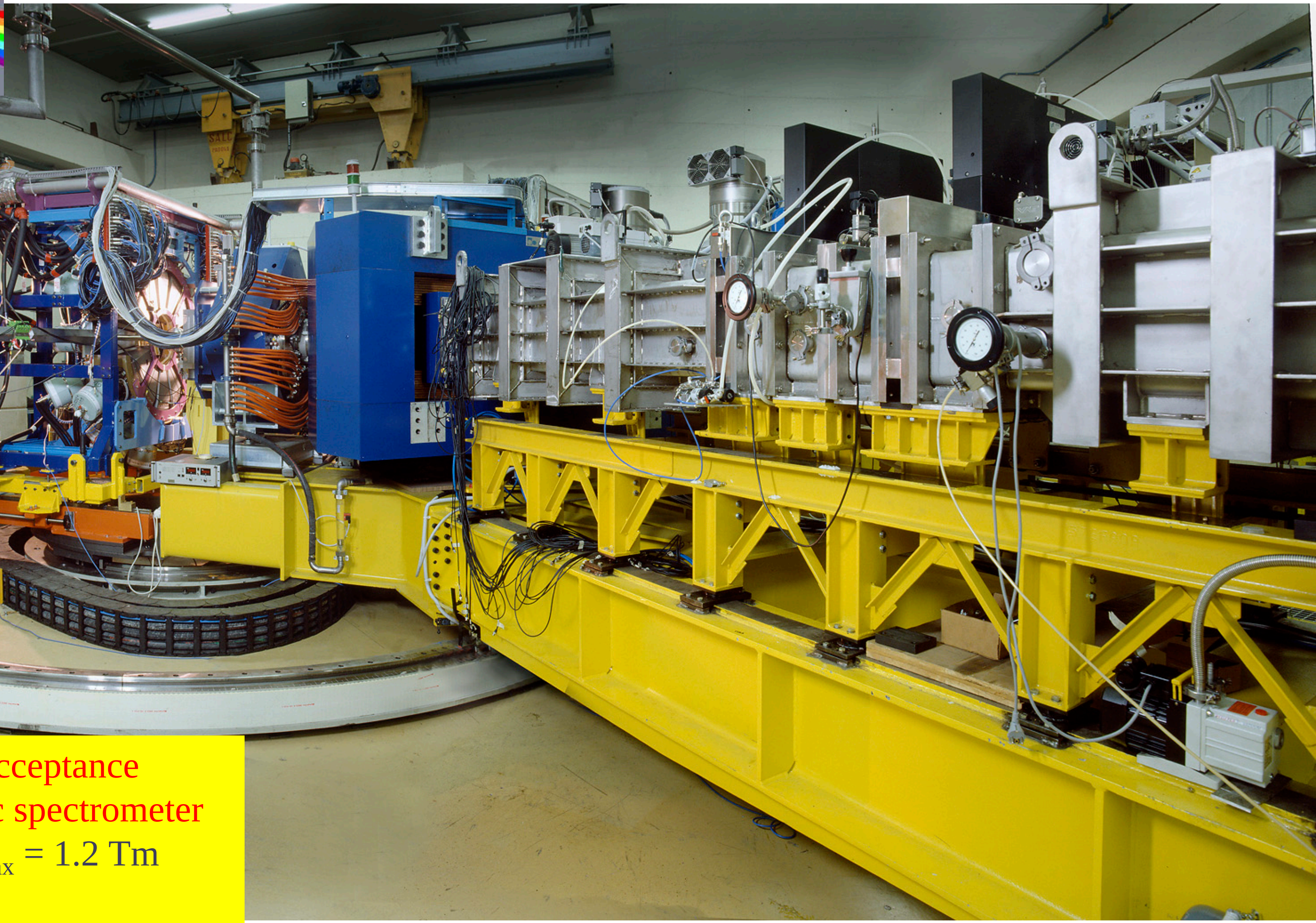

PRISMA: a large acceptance magnetic spectrometer

$\Omega \approx 80$ msr; $B\rho_{max} = 1.2$ Tm

$\Delta A/A \sim 1/200$

Energy acceptance ~ ±20%

Prisma spectrometer

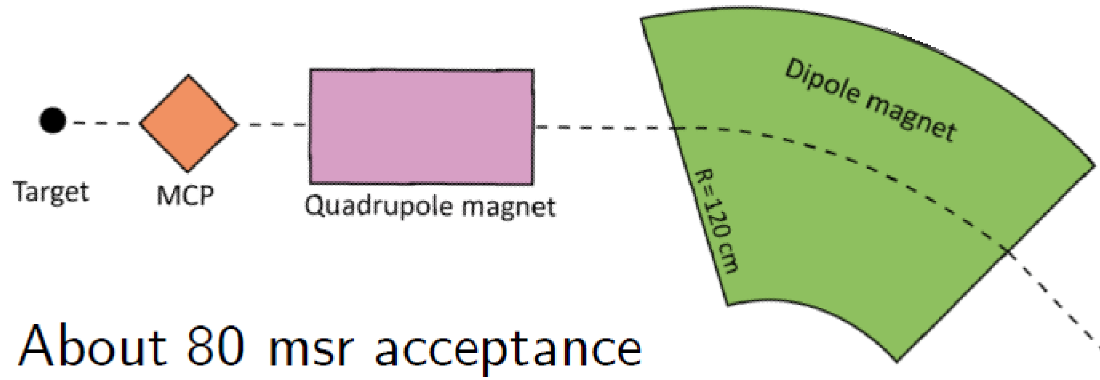

- About 80 msr acceptance
- Position sensitive detector systems
- Time of flight measurements
- Trajectory reconstruction
- Up to nuclei with A ≈ 140

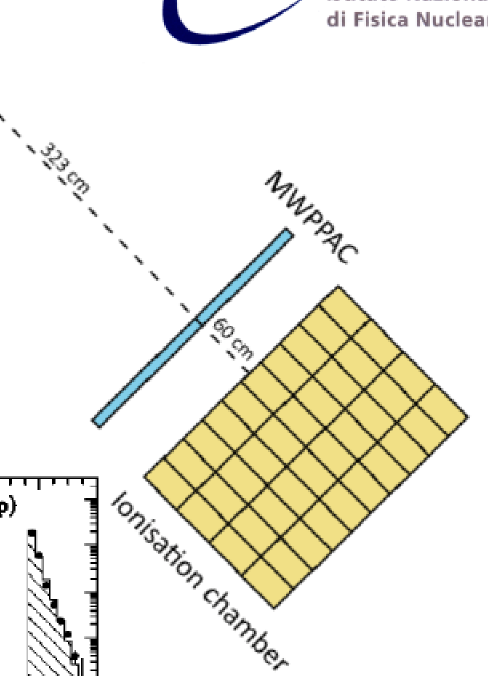

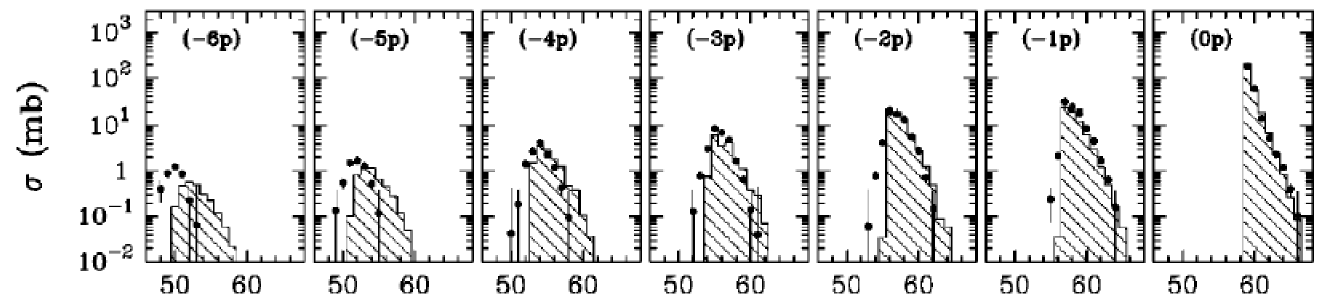

^{58}Ni + ^{208}Pb

Corradi, Phys. Rev. C 66, 024606 (2002)

MCP = micro channel plate

Heavy Ion Reaction Analyzer (HIRA)

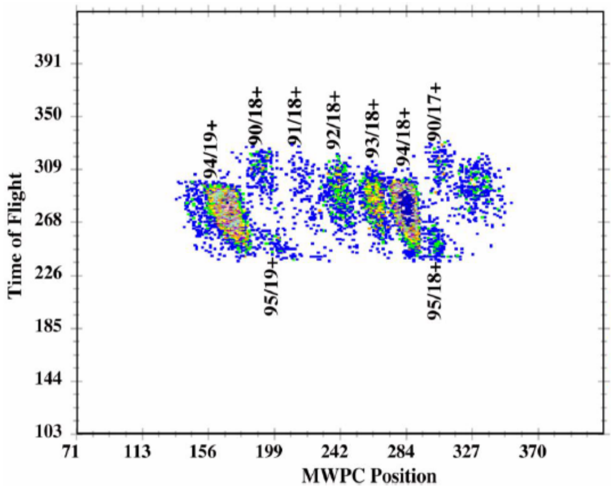

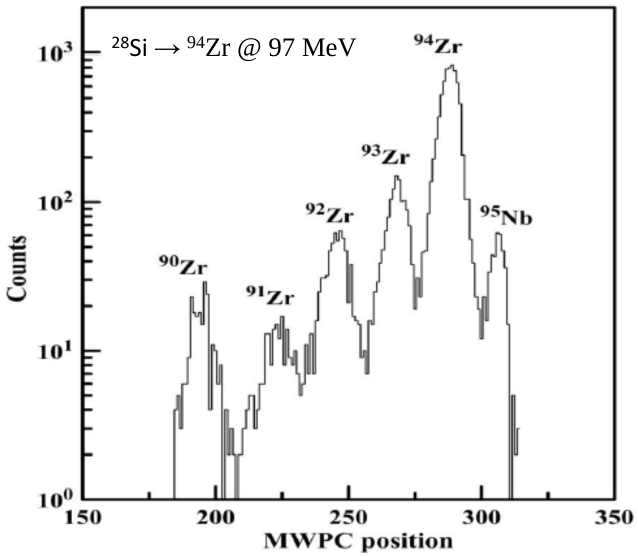

^{28}Si → ^{90,94}Zr @ E_{lab} = 83.3, 86.4, 89.5, 92.5, 95.5 MeV

^{28}Si → ^{90}Zr @ E_{cm} = 63.5, 65.9, 68.3, 70.6, 72.8 MeV V_C = 71.5 MeV
^{28}Si → ^{94}Zr @ E_{cm} = 64.2, 66.6, 69.0, 71.3, 73.6 MeV V_C = 71.1 MeV

S. Kalkal et al., Phys. Rev. C83 (2011) 054607

Why should we measure sub-barrier transfer?

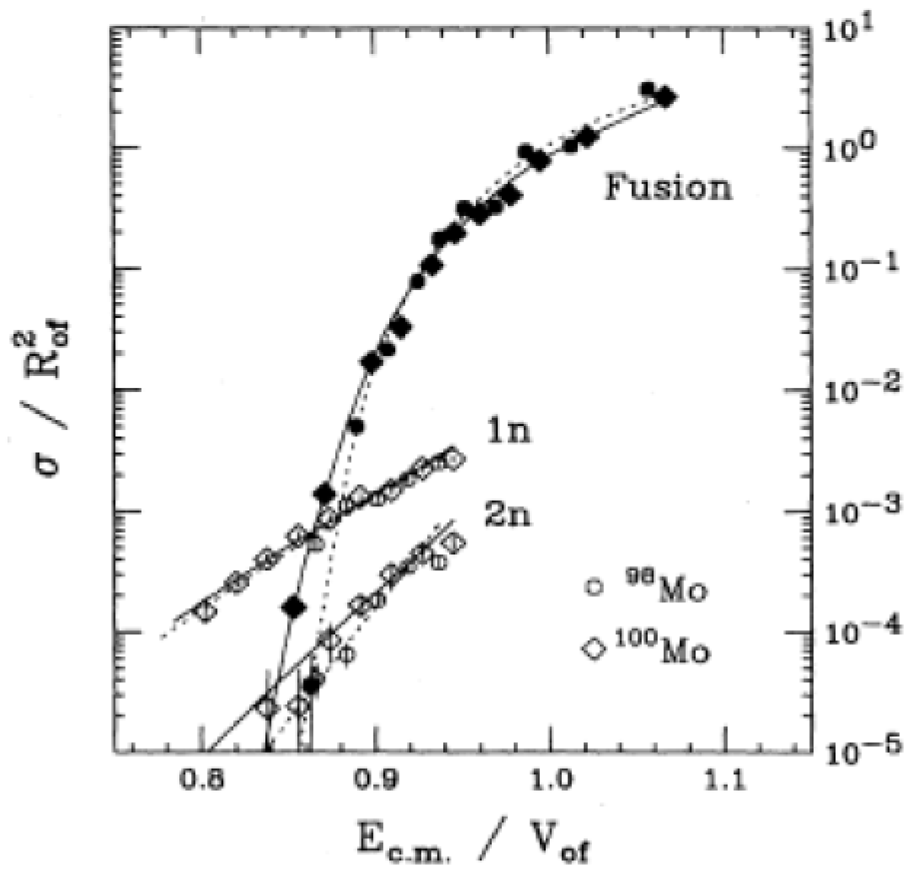

one probes transfer and fusion in an overlapping region of energies and angular momenta

^{7}Li

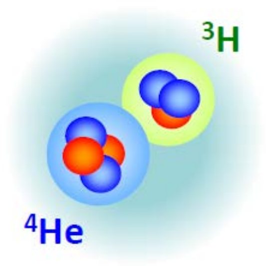

breakup threshold energy:

$Q_{breakup}$ = -2.467 MeV

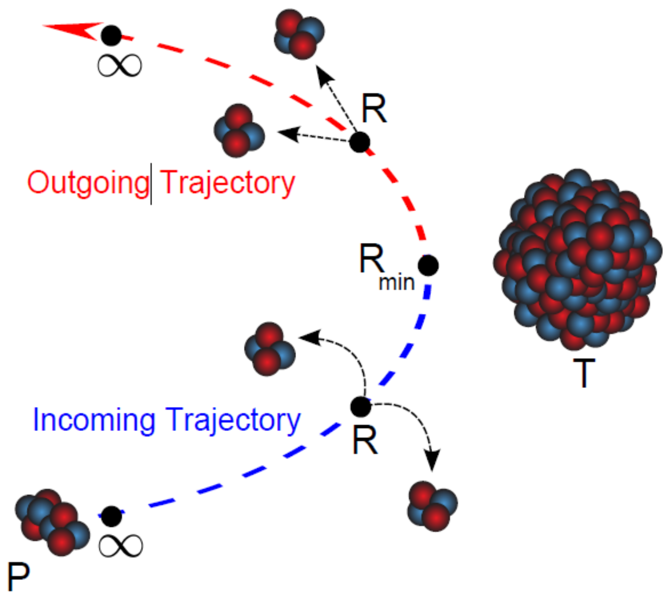

(^{7}Li,^{5}Li) -2n	(^{7}Li,^{6}Li) -1n	(^{7}Li,^{8}Li) +1n	(^{7}Li,^{9}Li) +2n	(^{7}Li,^{6}He) -1p	(^{7}Li,^{8}Be) +1p
-3.18 MeV	-2.65 MeV	-5.43 MeV	-8.25 MeV	-4.99 MeV	**+13.46 MeV**

$^{5}Li \rightarrow ^{4}He + ^{1}H$	$^{6}Li \rightarrow ^{4}He + ^{2}H$				$^{8}Be \rightarrow ^{4}He + ^{4}He$
+1.965 MeV	-1.474 MeV				+0.092 MeV

Structure and thresholds

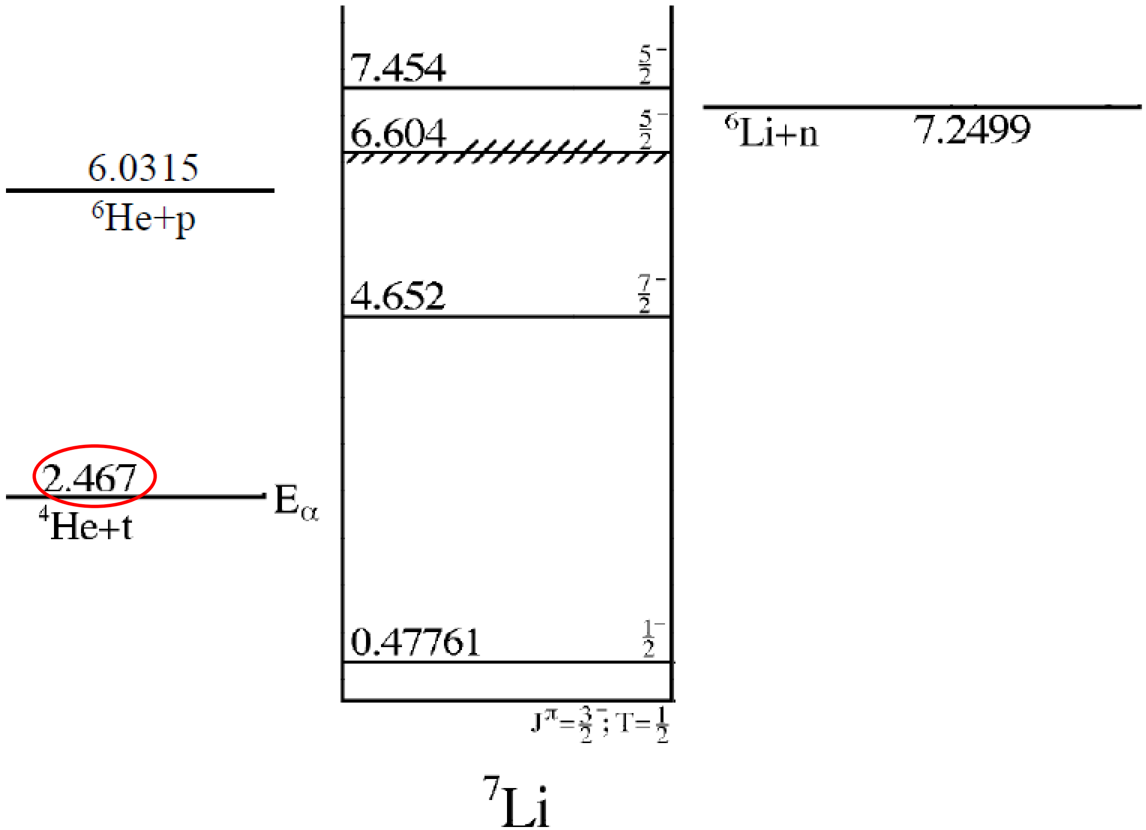

D. R. Tilley *et al*., Nucl. Phys. A490, 3 (1988)

Structure and thresholds

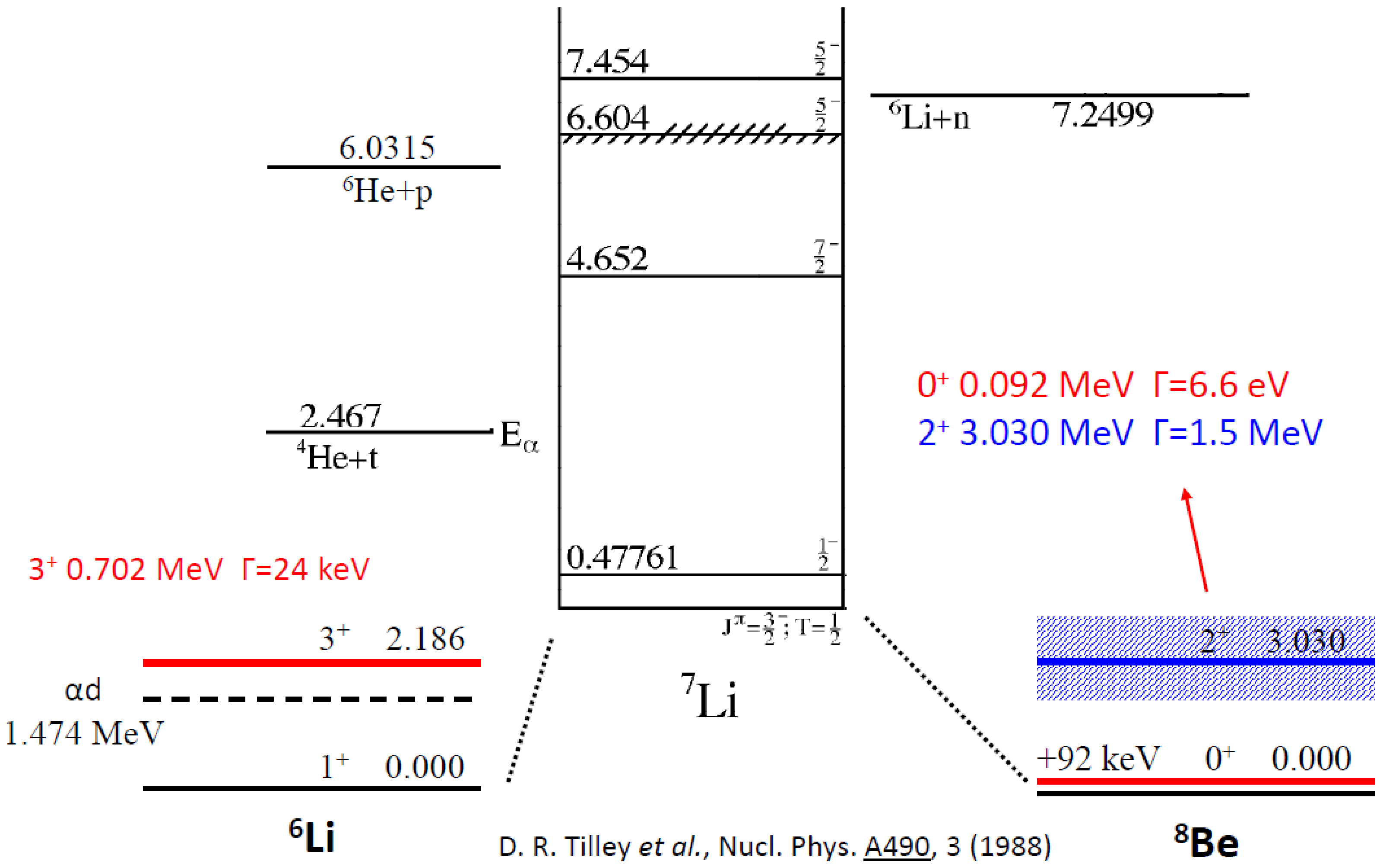

D. R. Tilley *et al.*, Nucl. Phys. A490, 3 (1988)

What causes the reduction in fusion?

^{7}Li

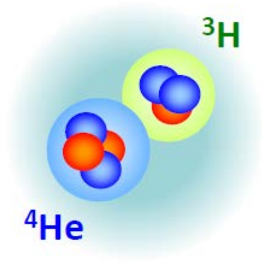

breakup threshold energy:
$Q_{breakup}$ = -2.467 MeV

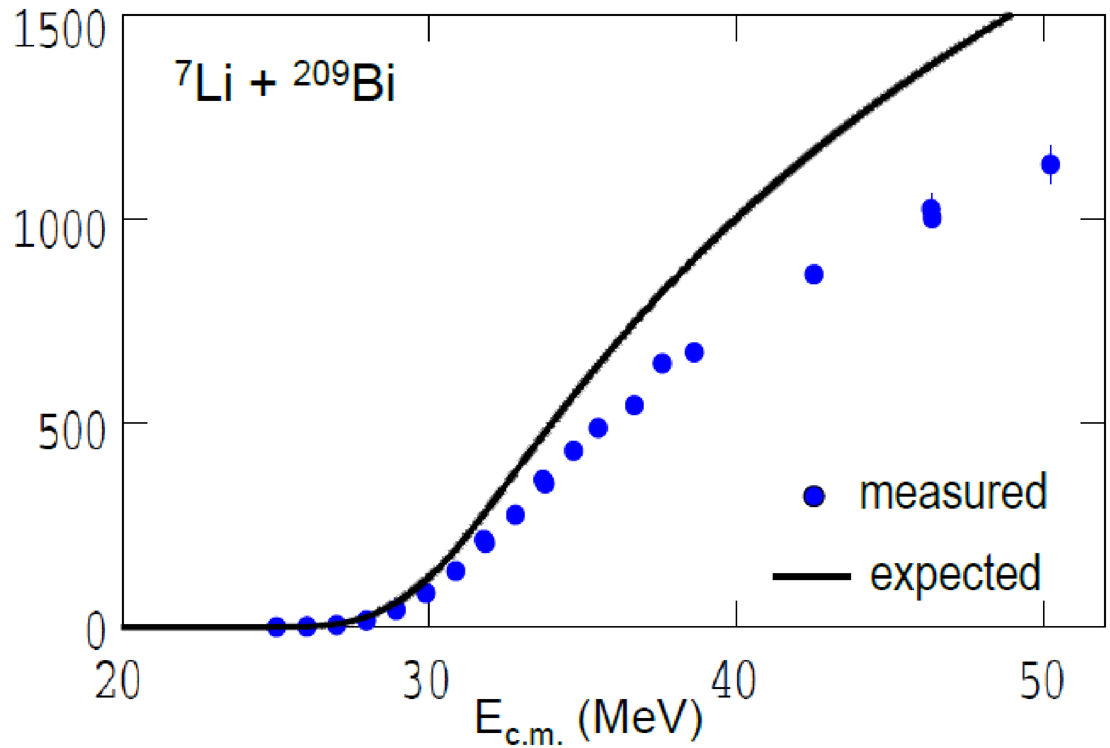

Dasgupta et al., Phys. Rev. Lett. 82 (1999) 1395

What causes the reduction in fusion?

^{7}Li

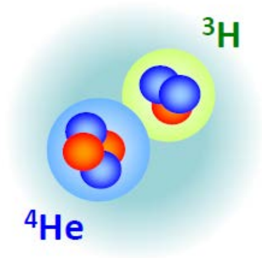

breakup threshold energy:
$Q_{breakup}$ = -2.467 MeV

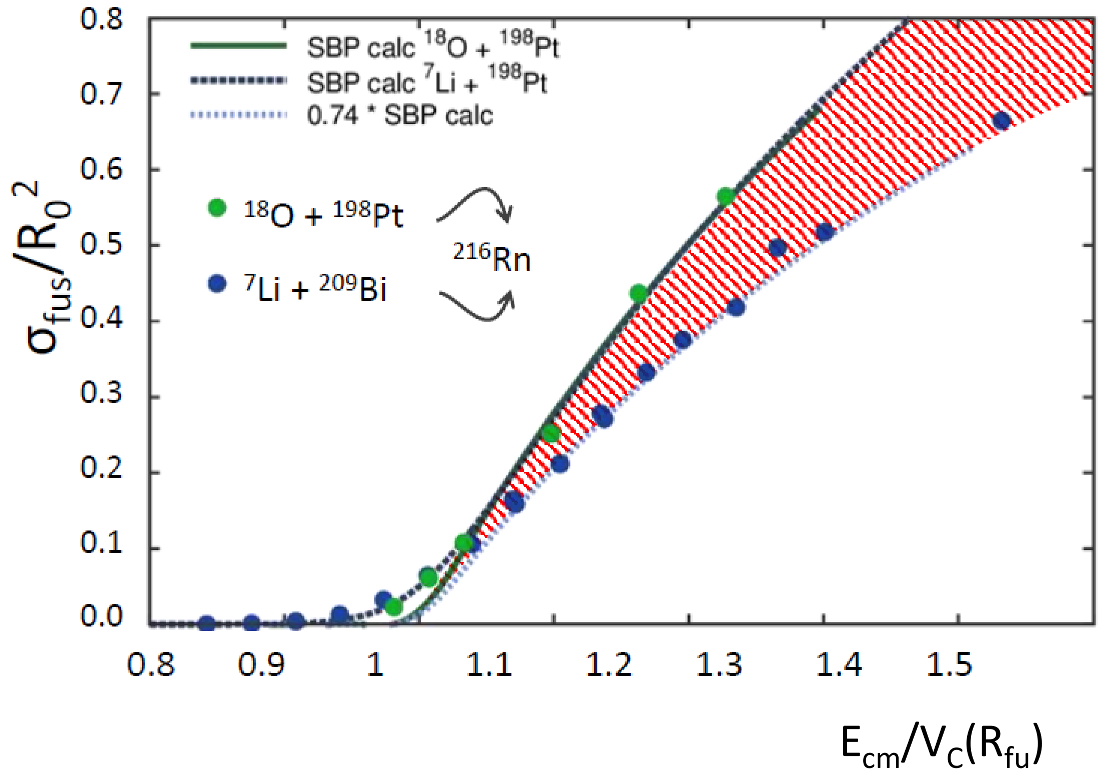

Fusion of weakly bound **^{7}Li + ^{209}Bi** suppressed relative to single-barrier calculation in contrast to **^{18}O + ^{198}Pt**

Dasgupta et al., Phys. Rev. C70, 024606 (2004)

Experimental set-up at ANU

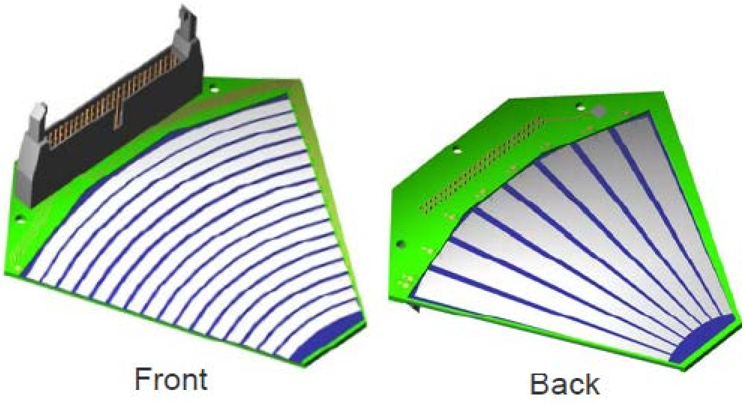

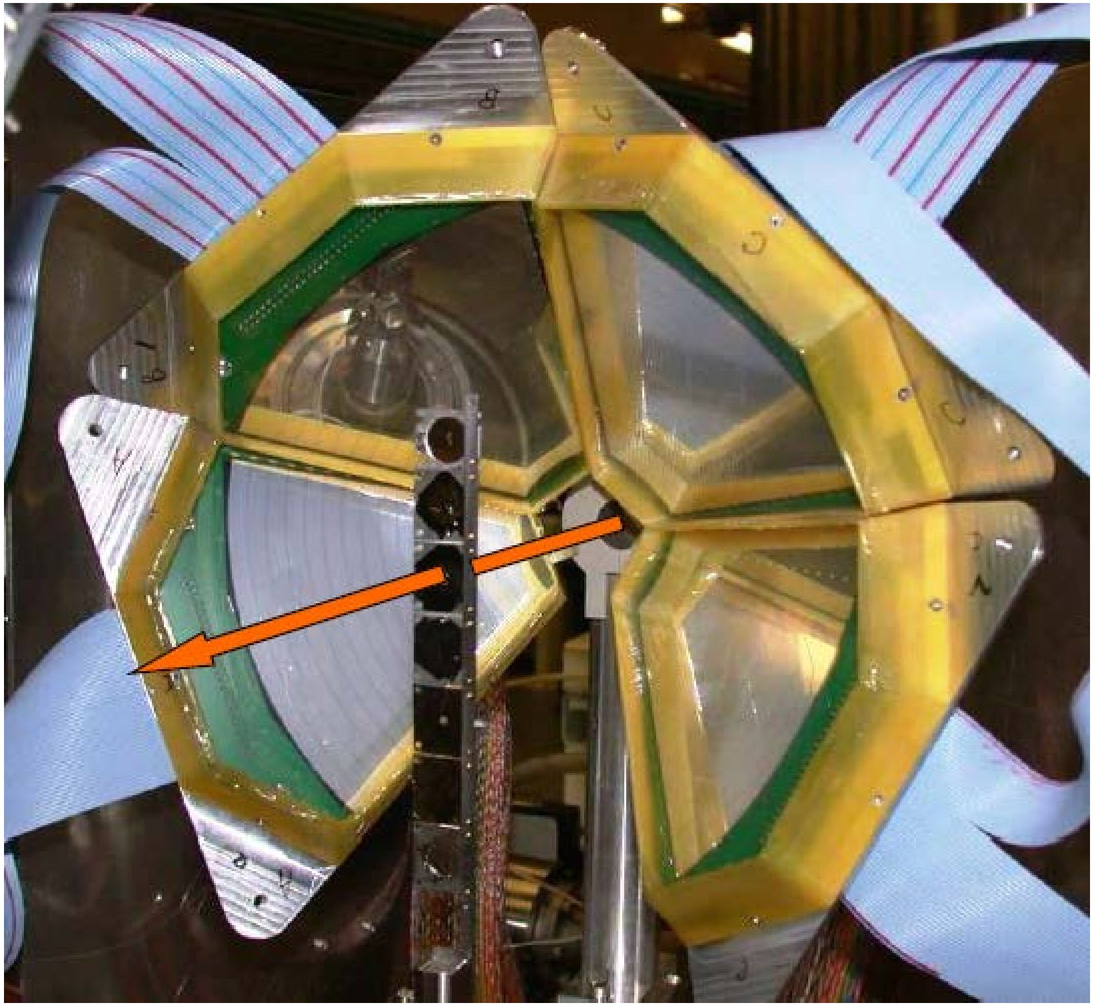

- 60^0 wedge detectors
  Micron semiconductor Ltd
- Large angular coverage (0.83 π sr)
- Detectors with high pixellation
  (512 pixels)

Reconstruction of Q-value non-relativistic implementation

1. energy conservation:

$$Q = (E_1 + E_2 + E_{recoil}) - E_{beam}$$

measured | from momentum conservation | known

2. momentum conservation (3-body breakup)

$$\vec{P}_{beam} = \vec{P}_1 + \vec{P}_2 + \vec{P}_{recoil}$$

$$E_{recoil} = \frac{\left|\vec{P}_{recoil}\right|^2}{2 \cdot m_{recoil}}$$

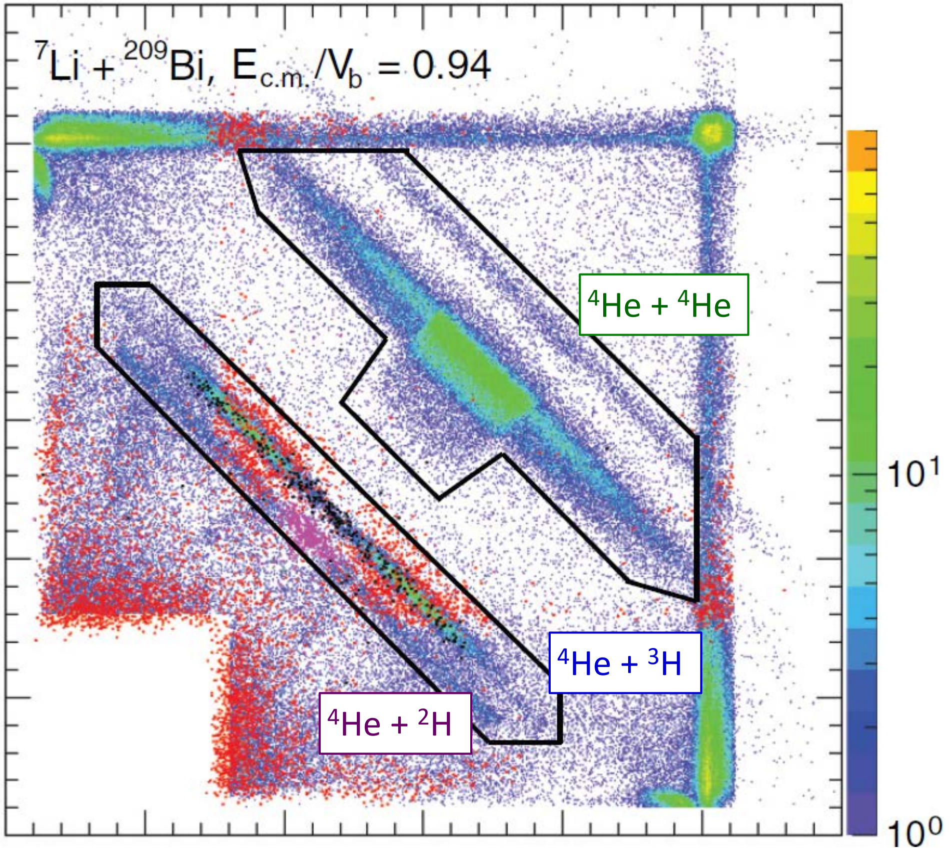

Q-value spectrum (target states)

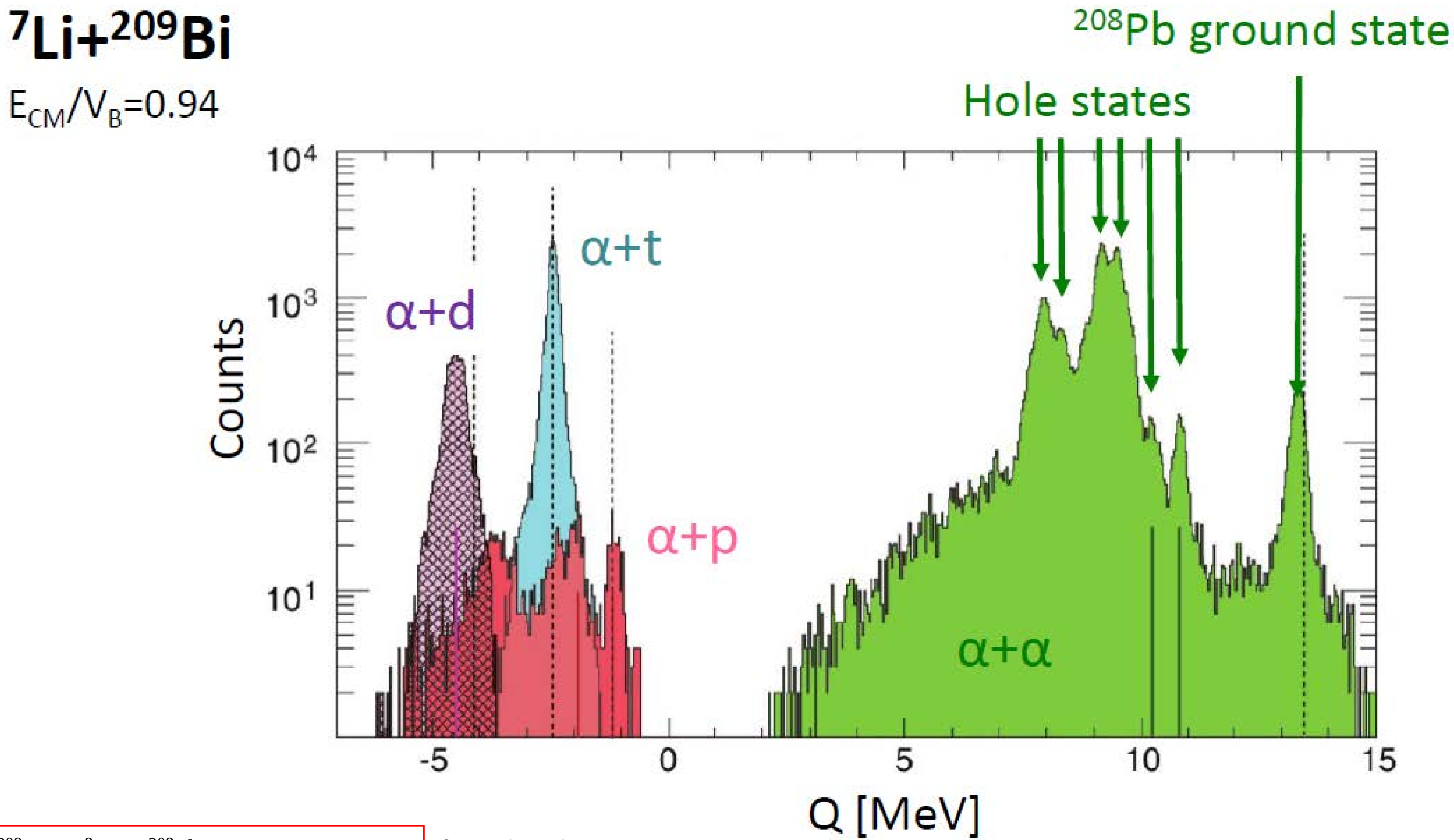

$^{7}Li + ^{209}Bi \rightarrow ^{8}Be + ^{208}Pb$	Q_{gg} = 13.457 MeV	$^{8}Be \rightarrow ^{4}He + ^{4}He$	Q_{gg} = +0.092 MeV
$\rightarrow ^{5}Li + ^{211}Bi$	Q_{gg} = -3.175 MeV	$^{5}Li \rightarrow ^{4}He + ^{1}H$	Q_{gg} = +1.965 MeV
$\rightarrow ^{6}Li + ^{210}Bi$	Q_{gg} = -2.645 MeV	$^{6}Li \rightarrow ^{4}He + ^{2}H$	Q_{gg} = -1.474 MeV

Q-value spectrum (target states)

$^{7}Li+^{208}Pb$

$E_{CM}/V_B=0.95$

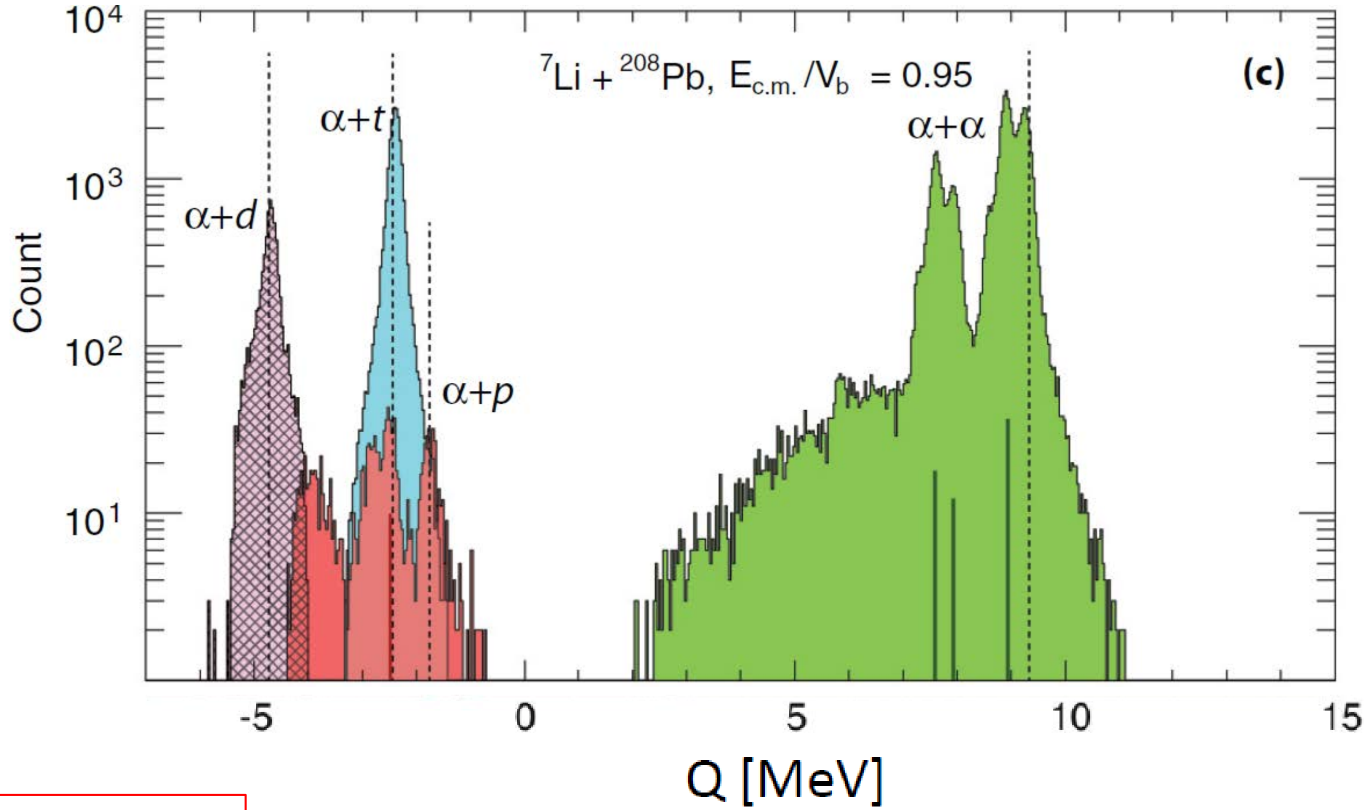

$^{7}Li + ^{208}Pb \rightarrow ^{8}Be + ^{207}Tl$ Q_{gg} = 9.246 MeV
$\rightarrow ^{5}Li + ^{210}Pb$ Q_{gg} = -3.792 MeV
$\rightarrow ^{6}Li + ^{209}Pb$ Q_{gg} = -3.313 MeV

$^{8}Be \rightarrow ^{4}He + ^{4}He$ Q_{gg} = +0.092 MeV
$^{5}Li \rightarrow ^{4}He + ^{1}H$ Q_{gg} = +1.965 MeV
$^{6}Li \rightarrow ^{4}He + ^{2}H$ Q_{gg} = -1.474 MeV

Q-value spectrum (target states)

$^{7}Li+^{207}Pb$

$E_{CM}/V_B=0.95$

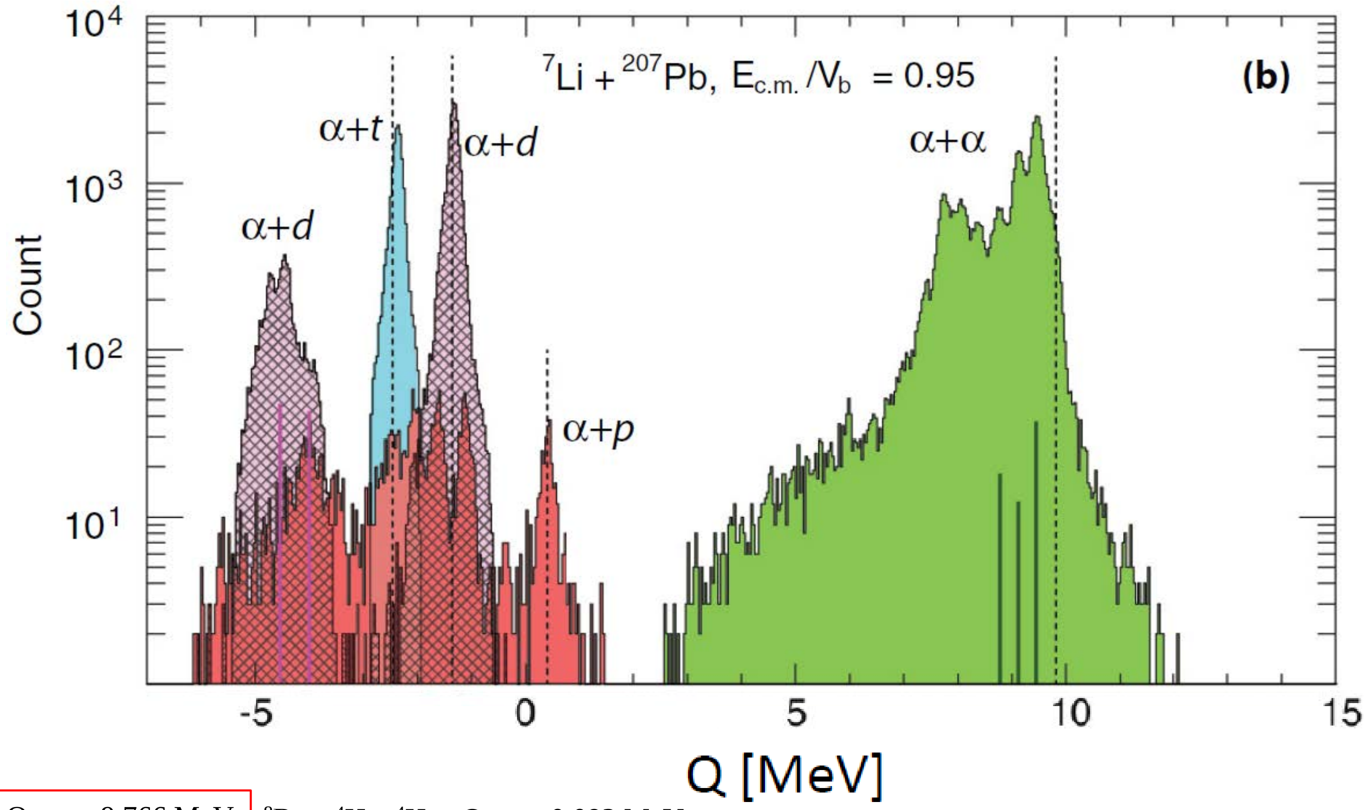

$^{7}Li + ^{207}Pb \to ^{8}Be + ^{206}Tl$ Q_{gg} = 9.766 MeV
$\to ^{5}Li + ^{209}Pb$ Q_{gg} = -1.610 MeV
$\to ^{6}Li + ^{208}Pb$ Q_{gg} = 0.118 MeV

$^{8}Be \to ^{4}He + ^{4}He$ Q_{gg} = +0.092 MeV
$^{5}Li \to ^{4}He + ^{1}H$ Q_{gg} = +1.965 MeV
$^{6}Li \to ^{4}He + ^{2}H$ Q_{gg} = -1.474 MeV